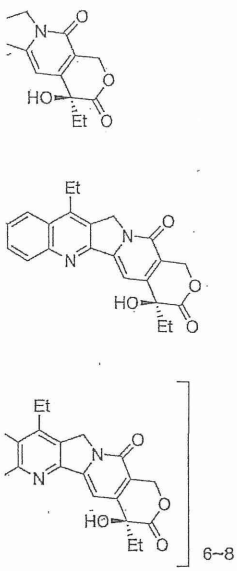

6–8

ates the cleavage site for

clots in cancer tissues
specific.

nt of CPT-11 which is
e mAb conjugation to
n, polyethylene glycol
own to evade nonspe-
er of drugs attached to

id SN-38 were evalu-
T-11 and three immu-
red to results in mice
itive and stroma poor)
IT2 tumors, while the
-CD20 immunoconju-
njugate, the tumor in

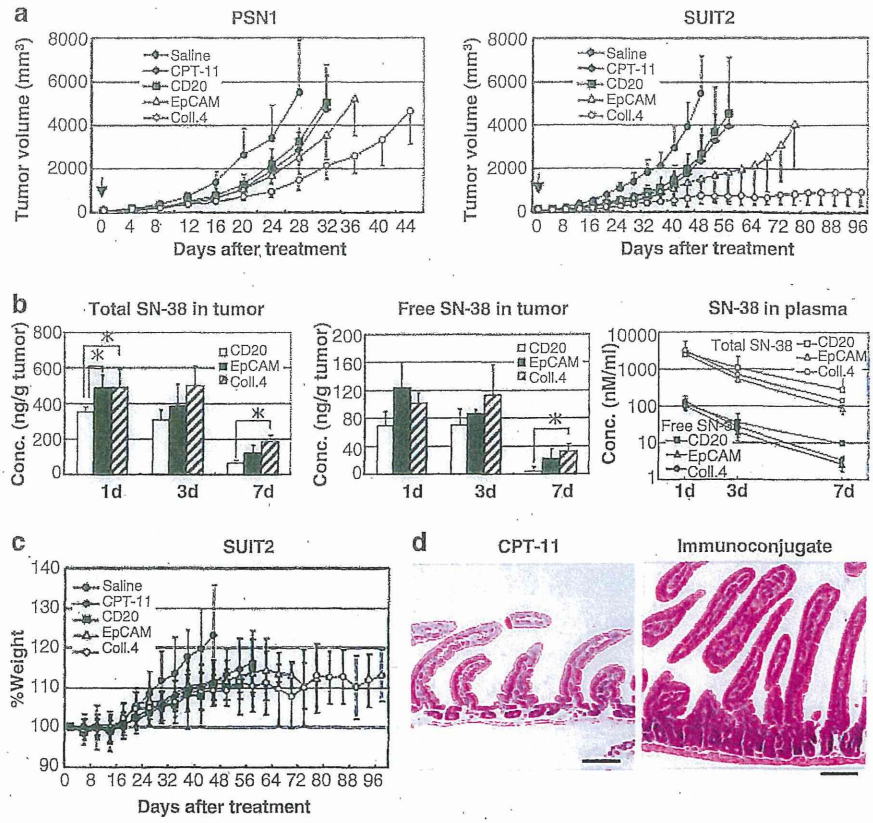

Fig. 6.5 Anti-tumor effects, pharmacokinetics and drug toxicities of anti-CD20, EpCAM and collagen 4 immunoconjugates. **(a)** Anti-tumor activities in vivo were examined. In animal models of PSN1 and SUIT2, the 3 immunoconjugates or saline as control, were administered to separate groups of mice by intravenous bolus injection on day. Arrows indicate day of administration and the curves illustrate the effects of the treatments on tumour size. $P<0.05$ (Saline or CD20 vs. EpCAM in PSN1), $P<0.01$ (Saline vs. CPT11 or EpCAM in PSN1, CPT11 or CD20 vs. EpCAM in SUIT2), $P<0.001$ (Saline vs. CPT11 or CD20 or EpCAM in SUIT2, Saline or CPT11 or CD20 or EpCAM vs. Collagen 4 in PSN1 or SUIT2). Bar=SD. **(b)** Tumor concentrations of total (bound and unbound) SN-38 (upper) and free (unbound) SN-38 (middle), and plasma concentrations (lower) were determined using HPLC analysis. The concentrations on days 1, 3 and 7 are shown. *$P<0.05$, Bar=SD. **(c)** Changes in the % body weight of saline, CPT-11, CD20, EpCAM and Collagen 4 in the same treated SUIT2 group (A) were shown Bar = SD. **(d)** Pathologic mucosal change of jejunum from mouse treated with CPT11 (upper) or anti-collagen 4 immunoconjugate (lower). Scale bar: 1mm. Coll.4,Collagen 4; Conc.,Concentration

mice treated with anti-collagen IV immunoconjugate stopped growing by about 1 month and never resumed up to 3 months (Fig. 6.5a). In mice bearing PSN1 tumors (stroma poor), differences were present but less marked. Thus, anti-collagen 4-SN-38 immunoconjugate exerted the most potent antitumor activity as compared with anti-CD20 or anti-EpCAM immunoconjugates and CPT-11 (Fig. 6.5a). In both

tumor models, anti-EpCAM immunoconjugate exerted superior antitumor effect compared to CPT-11 and anti-CD20 immunoconjugate, but inferior antitumor effect to anti-collagen IV immunoconjugate.

Significantly higher concentrations of free and total SN-38 were detected in tumor tissues of mice treated with the anti-collagen 4 immunoconjugate compared to the anti-CD20 immunoconjugate (Fig. 6.5b). The concentration of free and SN-38 in the tumor treated with anti-EpCAM immunoconjugate was intermediate among them, but not significant (Fig. 6.5b). There was no significant difference in body weight changes among saline groups, CPT-11, and immunoconjugate groups (Fig. 6.5c). In the small intestinal mucosa of mice, widespread villous atrophy and decreased crypt density were observed by the treatment of free unbound CPT-11 which is well known to have severe intestinal toxicity in clinics. On the other hand, the small intestinal mucosa of mice in groups treated with all immunoconjugates did not show any pathological change (Fig. 6.5d).

The most important observation from a therapeutic standpoint was that only SUIT2 tumors treated with anti-collagen IV immunoconjugate stopped growing about 1 month after treatment and remained dormant for more than 3 months. It may be concluded that the strategy of orchestrating slow sustained release from a scaffold erected on the stable inert structural components of the tumor stroma is most effective. We histologically compared this nongrowing tumor with a size-matched, growing, control tumor and found that both tumors showed central necrosis due to decreased blood flow, which is often observed in a murine xenotransplant model [38, 39]. The striking difference was that large confluent necrotic zones and dense fibrotic capsule formation were observed only in the treated tumor (Fig. 6.6a, b). In addition, CD31-positive endothelial cells, which may be tumor-feeding vessels in the peripheral part of the tumor, were never observed in the treated tumor compared with the untreated control. Instead, many collagen 4-positive round profiles corresponding to traces of destroyed vessels were observed in the peripheral area of the treated tumor (Fig. 6.6c).

CAST Therapy Using Anti-fibrin mAb

Chemically induced mouse cutaneous cancer was selected as an appropriate experimental model for evaluating the therapeutic effects of our immunoconjugate chemotherapy, because this spontaneous carcinogenetic model has remarkable fibrin deposition and abundant interstitial tissue as in human cancer (Fig. 6.7a), unlike human tumor xenografts, which have less fibrin clots and interstitial tissue [40, 41]. In addition, the spontaneous tumor is very slow in tumor growth that is also more similar to the general human cancer as compared to the xenografts. Using systemic in vivo imaging, anti-fibrin IgM, anti-fibrin chimeric IgG, and anti-fibrinogen IgG were delivered and retained in the tumor until day 3, utilizing leaky tumor vessels [1–3]. However, accumulation of anti-fibrin IgM and anti-fibrinogen IgG was weak

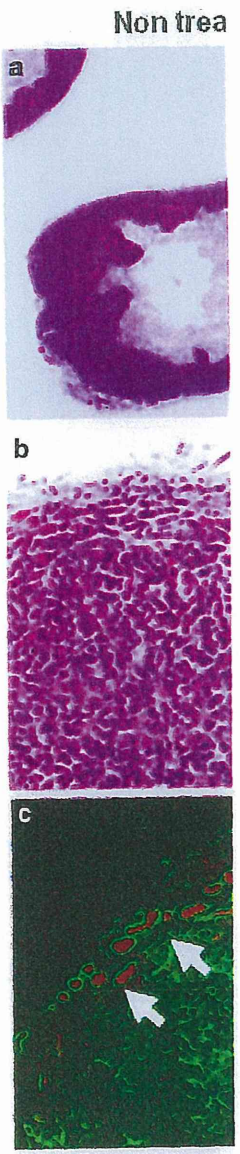

Fig. 6.6 Histopathologica
ment.(**a**) Hematoxylin an
SUIT2-tumors. A non-ne
The fibrotic capsule widt
vessels were examined b
arrows indicate tumor ves

perior antitumor effect
nferior antitumor effect

N-38 were detected in
moconjugate compared
centration of free and
ugate was intermediate
significant difference in
mmunoconjugate groups
ead villous atrophy and
f free unbound CPT-11
nics. On the other hand,
l all immunoconjugates

andpoint was that only
ugate stopped growing
re than 3 months. It may
ied release from a scaf-
e tumor stroma is most
or with a size-matched,
l central necrosis due to
e xenotransplant model
ecrotic zones and dense
tumor (Fig. 6.6a, b). In
mor-feeding vessels in
treated tumor compared
ve round profiles corre-
ie peripheral area of the

is an appropriate experi-
immunoconjugate che-
el has remarkable fibrin
ncer (Fig. 6.7a), unlike
terstitial tissue [40, 41].
growth that is also more
ografts. Using systemic
and anti-fibrinogen IgG
ing leaky tumor vessels
brinogen IgG was weak

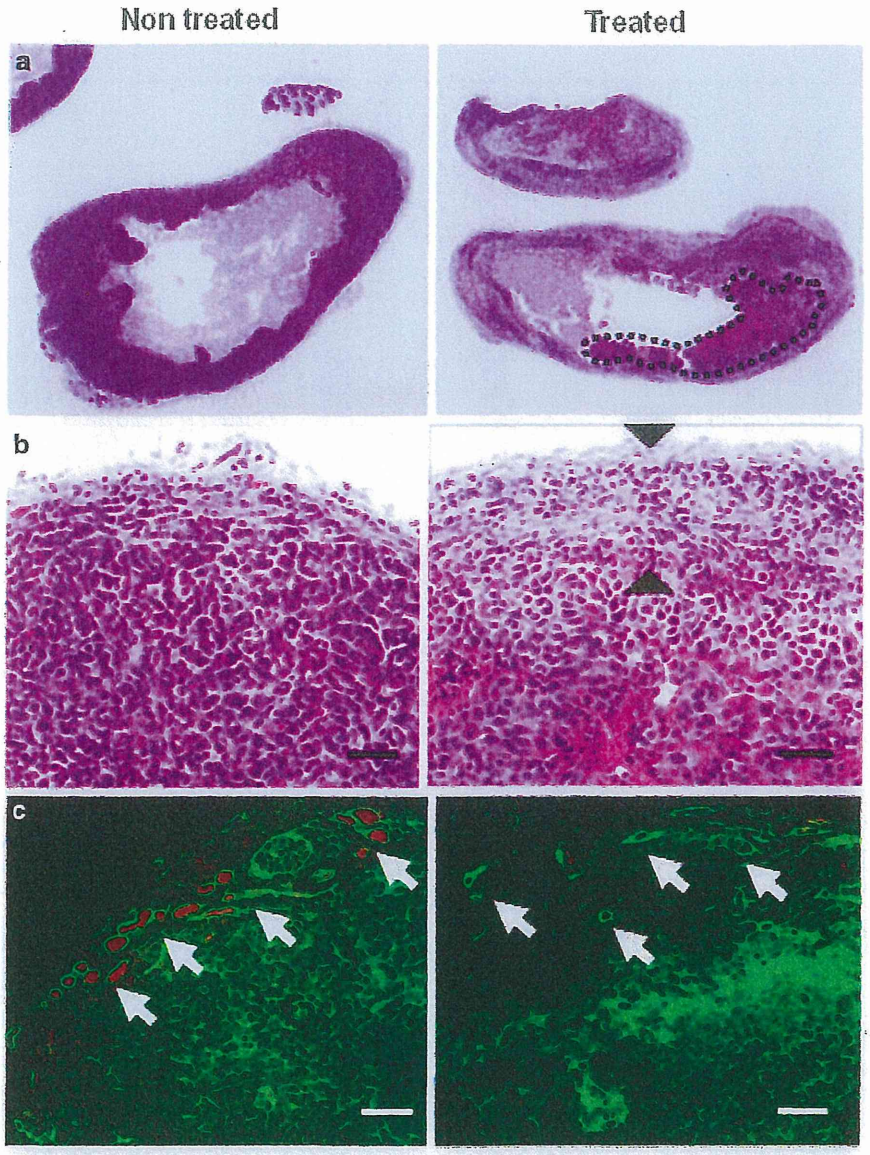

Fig. 6.6 Histopathological features of SUIT2 tumors after anti-collagen 4 immunoconjugate treatment.**(a)** Hematoxylin and eosin staining of non-treated (left) and immunoconjugate-treated (right) SUIT2-tumors. A non-necrotic viable lesion in the treated tumor is enclosed by a dotted line. **(b)** The fibrotic capsule width in the treated tumor is indicated between black arrowheads. **(c)** Tumor vessels were examined by the CD31 (red) collagen IV (green) double-staining techniques. White arrows indicate tumor vessels or their traces in the boundary area. Scale bar: 100μm

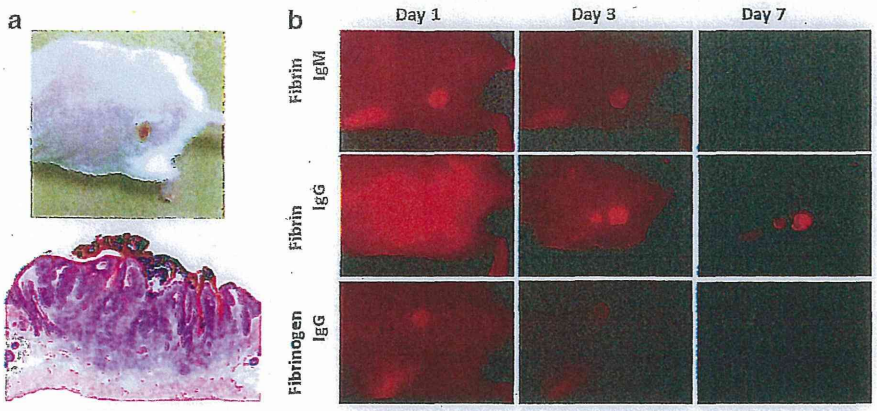

Fig. 6.7 **(a)** Chemical skin carcinogenesis. Mouse bearing a tumor (upper) and hematoxylin-eosin staining (lower) were shown. **(b)** In vivo systemic imaging analysis of Alexa-647-labeled anti-fibrin IgM (upper), Anti-fibrin chimeric mAb (middle) or anti-fibrinogen mAb (lower) on Days 1, 3 and 7 after injection. Arrows indicate each tumor position

and was eliminated by day 7, but the chimeric IgG was still highly retained (Fig. 6.7b). The use of human chimera is beneficial for clinical application to avoid human anti-mouse neutralizing antibodies (HAMA) and allergic reaction in human. In addition, because of the rapid blood clearance and low penetration of IgM compared with IgG [42], IgM is not suitable as a drug delivery vehicle. The branched composition had one maleimide for attachment of mAb, one PEG_{12} spacer, and three PEG_{27} ester bonds for attachment of three SN-38 molecules (Fig. 6.8a). There were approximately eight thiol residues able to react with the maleimide in the reduced mAb. The calculated drug (SN-38)/mAb ratio of the immunoconjugate was about 24. This immunoconjugate exerted significantly stronger antitumor activity compared with CPT-11 (Fig. 6.8b). Although treatment-related body weight loss was observed in mice treated with each drug, there was no significant difference between control groups and CPT-11 or the immunoconjugate treatment group. After injection of the immunoconjugate, the concentration of total SN-38 (antibody bound and unbound form) and free SN-38 (unbound form) in plasma gradually declined within a week, whereas CPT-11 showed rapid clearance (Fig. 6.9a). Significantly high concentrations of total and free SN-38 were detected in tumor tissues treated with the immunoconjugate for a long time compared to CPT-11 (Fig. 6.9b). The second significant observation of the treatment was a change in the gross tumor color from reddish to white (Fig. 6.9c). There was no clear change of fibroblast or macrophage, which plays an important role for tumor progression [43, 44]. It was found that discontinuation and irregularity comprising a mixture of narrowness and enlargement of the tumor vessels were manifested after treatment with the immunoconjugate (Fig. 6.9d, e).

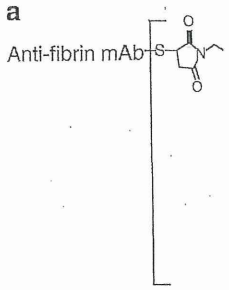

Fig. 6.8 Drug design, ant
immunoconjugate; anti-fibr
body bears 24 molecules of
SN-38. **(b)** Anti-tumor ac
were administered to mice
on Day 0, 7, 14, and 21. An
of treatment on tumor size
immunoconjugate). Bar =

We have made clea
immunoconjugate. Our
apy is unique as follow

1. Newly developed c
tumor vessels select
mal network.
2. The immunoconjug
from the scaffold, a
tumor.

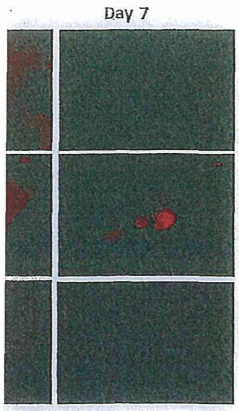

ɛr) and hematoxylin-eosin
f Alexa-647-labeled anti-
ı mAb (lower) on Days 1,

still highly retained
al application to avoid
gic reaction in human.
ıetration of IgM com-
vehicle. The branched
ne PEG_{12} spacer, and
ules (Fig. 6.8a). There
the maleimide in the
immunoconjugate was
ger antitumor activity
ıted body weight loss
significant difference
treatment group. After
N-38 (antibody bound
ma gradually declined
g. 6.9a). Significantly
ı tumor tissues treated
'T-11 (Fig. 6.9b). The
ge in the gross tumor
:hange of fibroblast or
ɛssion [43, 44]. It was
ure of narrowness and
nent with the immuno-

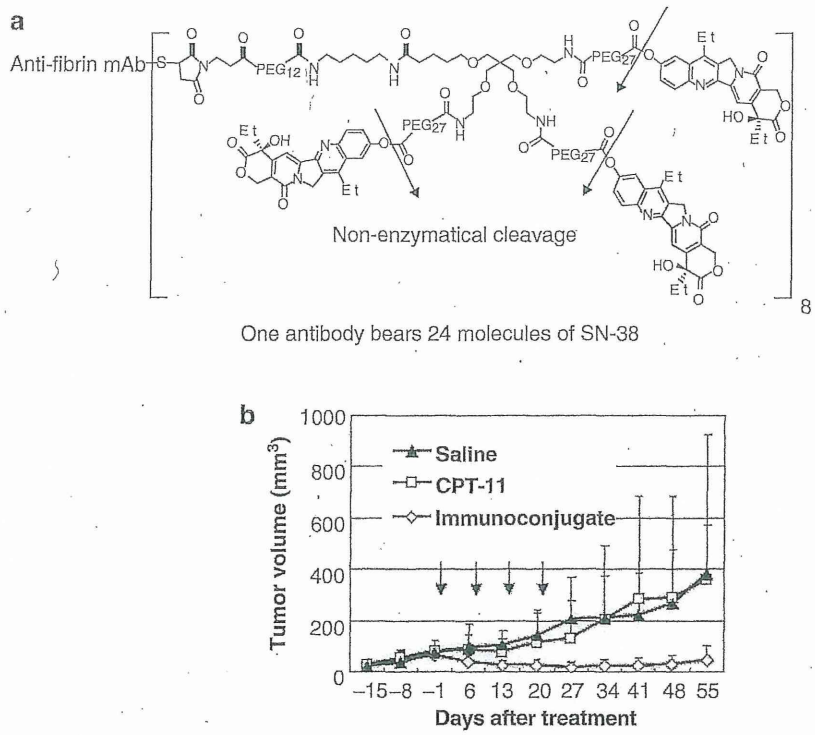

Fig. 6.8 Drug design, anti-tumor effect of anti-fibrin immunoconjugate (**a**) Drug design of immunoconjugate; anti-fibrin mAb-PEG-three branched PEG-(SN-38)3 via ester bond. One antibody bears 24 molecules of SN-38. The arrow indicates the cleavage site for releasing free active SN-38. (**b**) Anti-tumor activity in vivo was examined. Immunoconjugates, CPT-11 or saline, were administered to mice bearing chemical-induced cutaneous cancer via intravenous injection on Day 0, 7, 14, and 21. Arrows indicate day of administration and the curves illustrate the effect of treatment on tumor size. P =0.0005 (CPT-11 vs. immunoconjugate), P < 0.0001 (saline vs. immunoconjugate). Bar = SD

We have made clear that our newly developed tool is not a simple cytotoxic immunoconjugate. Our strategic concept of cancer stromal targeting (CAST) therapy is unique as follows.

1. Newly developed cytotoxic immunoconjugate can extravasate from the leaky tumor vessels selectively and forms a scaffold as it is captured by the tumor stromal network.
2. The immunoconjugate allows the effective sustained release of anticancer agent from the scaffold, and this released anticancer agent is distributed throughout the tumor.

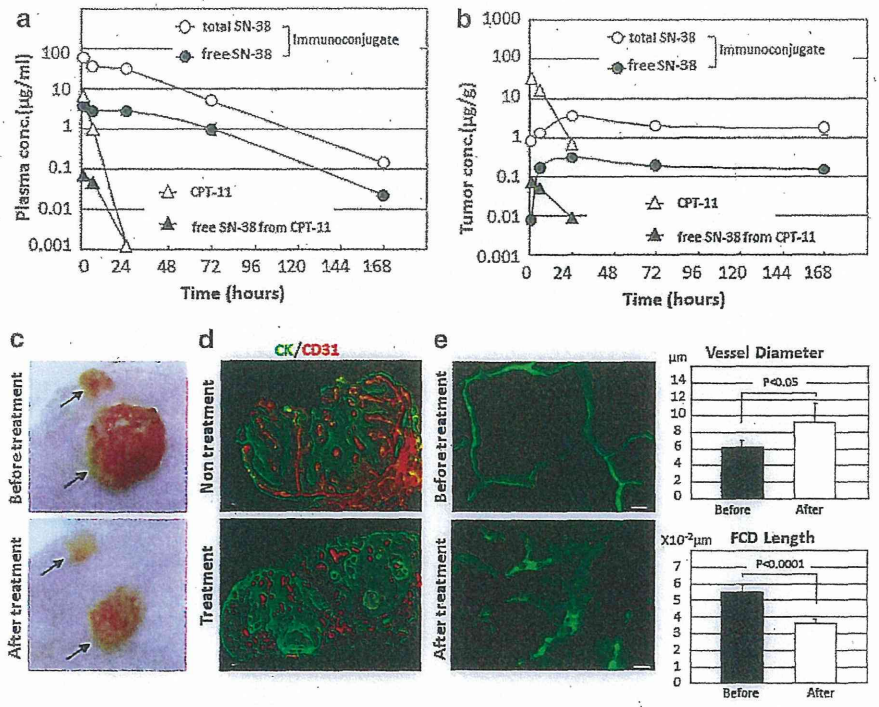

Fig. 6.9 Drug distribution and anti-vascular activity of anti-fibrin mAb conjugated with SN-38 (**a**) Plasma concentration of total SN-38 (bound and unbound form) or CPT-11 and free SN-38 (unbound form) released from the immunoconjugate or converted from CPT-11 was determined using HPLC analysis 1, 6, 24, 72, and 168 h after the injection. (**b**) Tumor concentration of total SN-38 (bound and unbound form) and free SN-38 (unbound form) released from the immunoconjugate, CPT-11 and free SN-38 converted from CPT-11 was determined using HPLC. (**c**) Tumor color changed from reddish to white at 5 days after injection of the immunoconjugate but not CPT-11. Arrows indicate each tumor position. (**d**) Tumor vessels after the injection of the immunoconjugate (Treatment) were examined using CD31 (red) and CK (cytokeratin, green). Untreated mouse (Non treatment) was used as control. bar: 100 μm. (**e**) Tumor vessels before and after the injection were visualized using FITC-dextran by in vivo fibered confocal fluorescence microscopy (left). Quantified vessel diameter and functional capillary density (FCD) length are shown (right). Bar: 20 μm

Consequently, the strategy described above was highly effective in causing arrest of tumor growth due to induced damage to tumor cells and tumor vessels without exerting the drug adverse effect (Fig. 6.10). Cancer stromal targeting therapy, utilizing a cytotoxic agent conjugated to a mAb directed at a specific inert constituent of the tumor stroma, is thus validated as a highly effective new modality of oncological therapy [45].

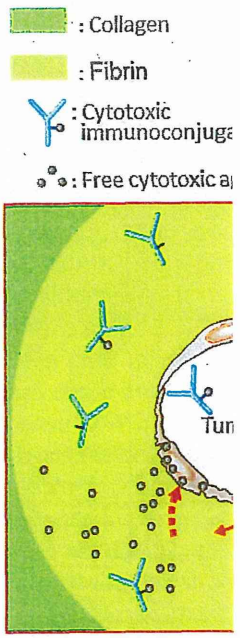

Fig. 6.10 Diagram of nev oped anti-fibrin mAb cor bind specifically to the fib the effective sustained rel Since this released anti-ca stroma barrier and induce

Tailored ADC De

Difference of Tun Lymphoma and P

Anti-collagen 4 mAb malignant lymphoma collagen-4-positive b spersed fibrously like tumor, SUIT2 tumor human pancreatic car collagen-4-positive e CD31-positive blood

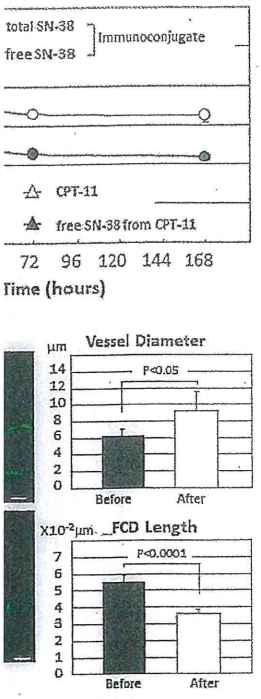

ıAb conjugated with SN-38
ı or CPT-11 and free SN-38
om CPT-11 was determined
Tumor concentration of total
eased from the immunocon-
ned using HPLC. (c) Tumor
e immunoconjugate but not
r the injection of the immu-
ytokeratin, green). Untreated
vessels before and after the
nfocal fluorescence micros-
ity (FCD) length are shown

ffective in causing arrest
d tumor vessels without
omal targeting therapy,
a specific inert constitu-
fective new modality of

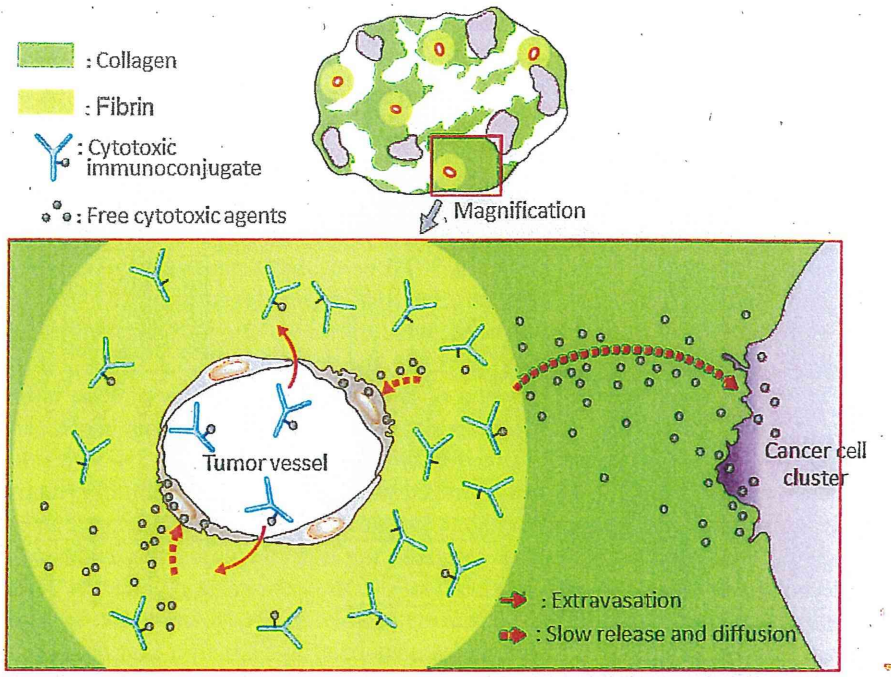

Fig. 6.10 Diagram of new concept of drug delivery using tumor stroma as a ligand. Newly developed anti-fibrin mAb conjugated with SN-38 extravasate selectively from leaky tumor vessels, bind specifically to the fibrin network around the tumor vessels to create a scaffold, and then allow the effective sustained release of SN-38, a time-dependent anti-cancer agent, from the scaffold. Since this released anti-cancer agent is LMW, it is subsequently distributed over the entire tumor-stroma barrier and induces damage not only to tumor cells but also to tumor vessels

Tailored ADC Depending on Quantity of Tumor Stroma

Difference of Tumor Stromal Component Between Malignant Lymphoma and Pancreatic Cancer

Anti-collagen 4 mAb was prepared to evaluate the stromal component. Human malignant lymphoma, RL tumor, consisted of CD20-positive tumor cells and collagen-4-positive blood vessels, which was stained fine linearly but not interspersed fibrously like the intercellular stroma. On the other hand, human pancreatic tumor, SUIT2 tumor reported as the histopathology relatively resembling original human pancreatic cancer [29, 46], consisted of EpCAM-positive cancer cells and collagen-4-positive extracellular component, the latter was composed of both CD31-positive blood vessel wall and high amount of CD31-negative stroma.

Preparation and Characterization of Cell-Targeting or Stroma-Targeting Immunoconjugate-PEG-SN-38 via a Carbamate Bond or Ester Bond

To specify the appropriate immunoconjugate therapy against malignant lymphoma or pancreatic cancer, we prepared two types of the conjugates, one being mAb-PEG-SN-38 via a carbamate bond [47] (Fig. 6.11a) and another being mAb-PEG-SN-38 via an ester bond [29, 30] (Fig. 6.11b). Consequently, six types of immunoconjugates, anti-CD20, anti-EpCAM, anti-collagen 4, or mAb-SN-38 via a carbamate bond or an ester bond, were obtained. The average number of conjugated SN-38 per one mAb (drugs/mAb), the range from 7 to 8.5, was shown in Fig. 6.11c. There was no clear loss of antigen-binding activity of each mAb after the conjugation (Fig. 6.11d). In in vitro release experiment, both bonds can be cut by a carboxylesterase localized in the cytoplasm to release SN-38 inside various cells (Fig. 6.11e). However, in physiological condition (non-enzymatically hydrolysis), the immunoconjugate prepared via an ester bond can release SN-38 gradually and effectively. In contrast, the immunoconjugate via a carbamate bond cannot release SN-38 effectively in the conditions outside the cells (Fig. 6.11e). We then evaluated the release profiles of SN-38 from both type of immunoconjugate in mouse blood, which contained high amounts of carboxylesterase [48]. In in vivo analysis of the mouse plasma, the concentration of unbound SN-38 or bound and unbound of SN-38 from the immunoconjugate via an ester bond or a carbamate bond at 72 h after the mice tail vein injection were shown. Most of the immunoconjugates in the mouse blood were protected from the enzymatic cleavage (Fig. 6.11f). Next, we examined the difference between carbamate bond and ester bond in the combination with cell-targeting or stromal-targeting antibody by the cytotoxicity assay. In RL cells, anti-CD20 immunoconjugate via carbamate bond showed strong cytotoxicity compared to anti-CD20 immunoconjugate via ester bond significantly (anti-CD20 mAb is known to possess high internalization ability). In SUIT2 cells, although no significant difference, anti-EpCAM immunoconjugate via carbamate bond had a lower tendency in the cytotoxic effect compared to anti-EpCAM immunoconjugate via ester bond (anti-EPCAM mAb is known to possess low internalization ability). Anti-collagen 4 immunoconjugate via ester bond showed higher cytotoxic activity than anti-collagen 4 immunoconjugate via carbamate bond in both cells significantly (Table 6.1). These results indicated that a carbamate bond was useful for the immunoconjugate linker to work inside of the cells and an ester bond to work outside the cells.

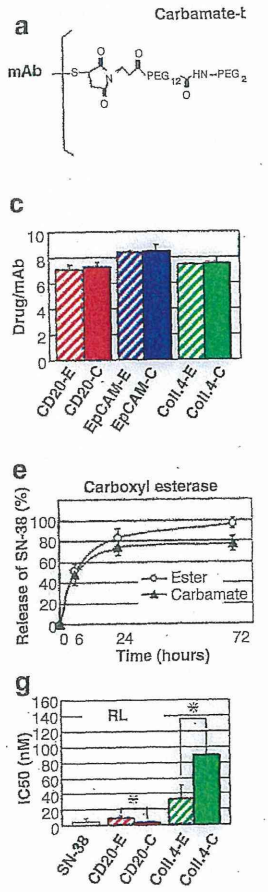

Fig. 6.11 Preparation and carbamate-bond and eser-b SN-38 via carbamate-bond molecules of SN-38. The a average number of conjug binding activity of the mAb mAb were examined by FA 4 mAb was examined by l types of immunoconjugate (right) (n=3). Bar=SD, *P unbound form of SN-38 fr after the mice tail vein inje HPLC. Bar=SD. (g) In vitr (right) was shown (n=3). B

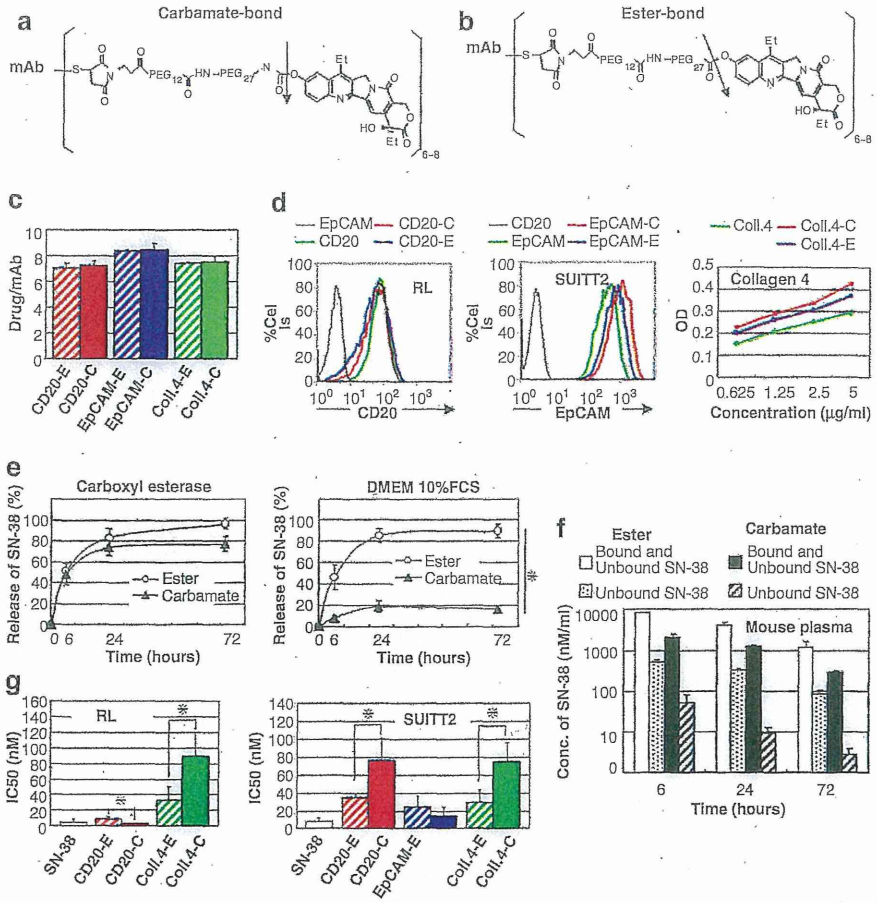

Fig. 6.11 Preparation and characterization of 2 types of immunoconjugqates-PEG-SN-38 via carbamate-bond and eser-bond. **(a)** **(b)** Drug design of 2 types of immunoconjugates; mAb-PEG-SN-38 via carbamate-bond **(a)** and mAb-PEG-SN-38 via ester-bond **(b)**. One antibody bears 6-8 molecules of SN-38. The arrow indicates the cleavage site for releasing free active SN-38. **(c)** The average number of conjugated SN-38 per one mAb was shown (n=3). Bar=SD. **(d)** Antigen-binding activity of the mAb before and after the conjugation was shown. Anti-CD 20 and EpCAM mAb were examined by FACS analysis using RL cells and SUIT2 cells respectively. Anti-collagen 4 mAb was examined by ELISA using purified protein. **(e)** In vitro release of SN-38 from two types of immunoconjugates in carboxylesterase-contained solution (left) and DMEM 10%FCS (right) (n=3). Bar=SD, *P<0.05. (f) Concentration of bound and unbound form of SN-38, and unbound form of SN-38 from two types of immunoconjugates in the moue plasma at 6, 24, 72 h after the mice tail vein injection, were shown (n=3). Concentrations of SN-38 were determined by HPLC. Bar=SD. **(g)** In vitro cytotoxicity with immunoconugates in RL cells (left) or SUIT2 cells (right) was shown (n=3). Bar=SD, *P<0.05

Table 6.1 IC50 of free SN-38 and SN-38 conjugated to mAb (immunoconjugate) for malignant lymphoma and pancreatic cancer cell line

		SN-38 conjugated to mAb					
Malignant lymphoma cell lines	Free SN-38	CD20				Collagen 4	
		Ester	Carbamate			Ester	Carbamate
RL	4.6±3.7	8.7±2.9 vs. 2.1±1.0*				34±17 vs. 90±30*	
		SN-38 conjugated to mAb					
Pancreatic cancer cell lines	Free SN38	CD20		EpCAM		Collagen 4	
		Ester	Carbamate	Ester	Carbamate	Ester	Carbamate
SUIT2	7.8±3.6	35±5 vs.	77±25*	24±13 vs.	15±9	29±15 vs.	75±22*

IC50 (50% cell survival) (nM), Mean±standard deviation (n=3), *P<0.05

Cell-Targeting or Stroma-Targeting Immunoconjugate-PEG-SN-38 via Carbamate Bond or Ester Bond Differs Drastically in Their Antitumor Effects Depending on Tumor Stromal Component in Mice

Three mAbs conjugated with SN-38 via carbamate bond or ester bond (administered once, at an equivalent SN-38 dose of 3 mg/kg) were evaluated in order to know their antitumor effects in RL (CD20-positive stroma-poor human malignant lymphoma), SUIT2 (EpCAM-positive stroma-rich human pancreatic tumor). In RL lymphomas, cell-targeting anti-CD20 mAb-SN-38 via carbamate bond showed superior antitumor activity compared to anti-CD20 mAb-SN-38 via ester bond after the treatment (Fig. 6.12a). Stroma-targeting anti-collagen 4 mAb-SN-38 via ester bond showed significant superior antitumor activity as compared to saline as control, but inferior to anti-CD20 mAb-SN-38 via carbamate bond (Fig. 6.12a). On the contrary to RL tumor, in SUIT2 tumor, the most potent antitumor activity was obtained by the stroma-targeting anti-collagen 4 mAb-SN-38 via ester bond (Fig. 6.12b). However, there was no significant difference of antitumor activity between anti-EpCAM mAb-SN-38 via carbamate bond and via ester bond, whereas the antitumor activity of anti-collagen 4 mAb-SN-38 via carbamate bond was inferior to that of anti-collagen 4 mAb-SN-38 via ester bond (Fig. 6.12b). These results clearly indicated that in stroma-poor solid tumors like malignant lymphoma, cytotoxic immunoconjugate should target to the tumor cell surface and ACA should be conjugated to mAb through carbamate bond which can be specifically cut by a carboxylesterase inside the tumor cell after the internalization. On the other hand, in stroma-rich tumors, the immunoconjugate should target to the stroma within tumor tissue and ACA should be attached to the mAb via ester bond which can be cut gradually outside the tumor cell following the accumulation of the cytotoxic immunoconjugate in

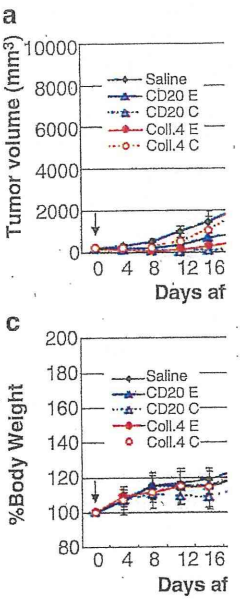

Fig. 6.12 Antitumor effe anti-stroma targeting, carl cent changes of body wei the 6 types of immunocon or anti-collagen 4 mAb=C administered once at an e intravenous bolus injectic curves illustrate the effec CD20-C vs. CD20-E, C Coll.4-E, Coll.4-E vs. Ep (Saline vs. Coll.4-E in R Bar=SD

the tumor stroma. It influence the outcome mAb-PEG-SN-38 vi via ester bond.

Regarding normal there was no differenc The dose in this study mouse body weight (I toxicity, or bone mar as compared to cont adverse effects such a anti-collagen 4 mAb, ride caused severe art